Available online at www.sciencedirect.com
ScienceDirect
Journal of Organometallic Chemistry 692 (2007) 3454–3460
Journal of Organometallic Chemistry
www.elsevier.com/locate/jorganchem

Reaction mechanisms of Cp-containing silene complexes toward H_2: A DFT study

Siwei Bi [a,*], Shufen Zhu [a], Zhenwei Zhang [a], Zhaodong Yuan [b]

[a] College of Chemistry Science, Qufu Normal University, Qufu, Shandong 273165, PR China
[b] Department of Chemistry, Teachers College of Jining, Qufu, Shandong 273155, PR China

Received 4 March 2007; received in revised form 5 April 2007; accepted 11 April 2007
Available online 21 April 2007

Abstract

The 18e Cp-containing silene tungsten complex, $Cp_2W(\eta^2\text{-}Me_2Si{=}CH_2)$, can break H–H bond to afford the product, $Cp_2WH(SiMe_3)$. The mechanisms on reaction of $Cp_2W(\eta^2\text{-}Me_2Si{=}CH_2)$ with H_2 are investigated in this paper by using density functional theory (DFT). On the basis of the features of the reaction and experimental proposal for the reaction mechanisms, three possible pathways are proposed, which are related to the migration of silicon group, Cp ring slippage, and σ-bond metathesis, respectively. Our results of calculations indicate that the pathway involving migration of silicon group is the most favored, supporting the experimental observations. The other two paths are quite unfavorable kinetically.

Keywords: Silene tungsten complex; Ring slippage; Insertion; Mechanism

1. Introduction

Transition metal can stabilize reactive species by ligation. Silenes ($R_2C{=}SiR'_2$) are usually reactive, but stable transition metal silene complexes could be synthesized and isolated. In 1988 and 1990, Tilley and co-workers respectively isolated and studied $Cp^*(PR_3)Ru(H)\text{-}(\eta^2\text{-}CH_2{=}SiPh_2)$ ($Cp^* = \eta^5\text{-}C_5Me_5$; R = ^{i}Pr; Cy) [1] and $Cp^*(PMe_3)Ir$ ($\eta^2\text{-}CH_2{=}SiPh_2$) [2]. At almost the same time, Berry and co-workers prepared a tungsten silene complex $Cp_2W(\eta^2\text{-}Me_2Si{=}CH_2)$ [3] in 1990. The investigations on silene complexes have also been reported by others [4–9].

Normally, small member silametallacycles, particularly three-membered ring compounds have strained molecular structures, peculiar bonding modes, and novel reactivity [10,11]. Quite interestingly, as predicted in experiments, reactions of Cp-containing silametallacyclopropane toward certain substrates, such as H_2 and $HSiMe_3$, undergo migration of silyl group, leading to slippage of Cp ring from η^5 to η^4 coordination mode [3,12]. Reaction (1) shows $Cp_2W(\eta^2\text{-}Me_2Si{=}CH_2)$ (denoted as **R**) can break the H–X (X = H, $SiMe_3$) bonds to form W–X bonds. This reaction is featured by (i) migration of silicon group which is supported by the reaction of $Cp_2W(\eta^2\text{-}Me_2Si{=}CH_2)$ with ethylene [3], (ii) slippage of Cp ring from η^5 to η^4 coordination mode, and (iii) 18e configuration of **R**. Theoretical study on such kind of reactions is still rather limited. On the basis of the features mentioned above, together with the experimental observations, three possible pathways are proposed in this work. The first pathway undergoes migration of the $SiMe_2$ from W to Cp ring, which was proposed by Berry and co-workers [3,12]. Such kind of reactions involving silicon group migration was also reported in the literatures [13–15]. Ring slips are common in late transition metal Cp complexes [16]. For example, Casey and co-workers predicted that the Cp ring could undergo ring slip from η^5 to η^3 to η^1 coordination in the conversion of $[\eta^5\text{-}CpRe(CO)_3]$ to $[\eta^1\text{-}CpRe(CO)_3(PMe_3)]$ [17]. The second pathway is based on such a Cp ring slippage which

* Corresponding author. Fax: +86 537 4456305.
E-mail address: siweibi@126.com (S. Bi).

0022-328X/$ - see front matter © 2007 Elsevier B.V. All rights reserved.
doi:10.1016/j.jorganchem.2007.04.012

reduces the electron count of the metal by two electrons, permitting dihydrogen to coordinate without having to proceed through an unfavorable 20-electron intermediate. Considering the reactant **R** is 18e and no neutral ligand is attached to the metal, we propose the third pathway, a σ-bond metathesis process [18,19].

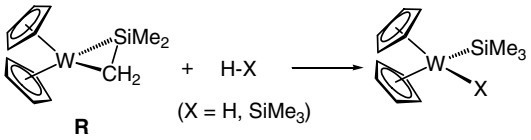

(1)

In this paper, our goal is to investigate the mechanisms of reaction (1) with the support of the Berry's proposal and experimental observations. We expect this work could enhance further understanding and provide helpful information for chemists for further exploration of such kind of reactions.

2. Computational details

All molecular geometries were optimized at the Becke3-LYP (B3LYP) level of density functional theory (DFT) [20–22]. Frequency calculations at the same level of theory have also been performed to identify all stationary points as minima (zero imaginary frequencies) or transition states (one imaginary frequency). The transition states involved were checked by IRC (intrinsic reaction coordinate) analysis [23,24]. The effective core potentials (ECPS) of Hay and Wadt with double-ζ valence basis sets (LanL2DZ) [25] were used to describe W and Si atoms, while the standard 6-31G basis sets were used to describe C and H atoms. Polarization functions were added for Si ($\zeta(d) = 0.262$) and those atoms directly involved in bond-forming and bond-breaking processes, C ($\zeta(d) = 0.8$), H ($\zeta(p) = 0.11$). All the calculations were performed with the GAUSSIAN-98 software package.

The computational method and the basis sets used in this work have been extensively recognized in theoretically investigating structures, bonding and reaction mechanisms of organometallic systems [26]. For examining the feasibility of the B3LYP level of density functional theory, the computed geometrical structure of the reactant (**R**) was compared with the original X-ray diffraction structure. Selected calculated and experimental bond distances were shown in Table 1. Calculated and X-ray geometrical parameters were close enough, indicating our calculations at the B3LYP level of density functional theory were reliable.

Table 1
Selected bond distances (Å) for **R**

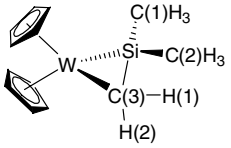

	Calculated data	Experimental data
W–Si	2.58	2.53
W–C3	2.33	2.33
Si–C1	1.90	1.90
Si–C2	1.90	1.88
Si–C3	1.83	1.80

3. Results and discussion

In this work, we choose the typical reaction of **R** with H_2 as a model reaction to explore the reaction mechanisms. On the basis of the features discussed in Section 1, three possible pathways of the reaction are proposed as shown in Scheme 1.

Path I is given based on Berry and co-worker's proposal where the silicon migration is involved. $SiMe_2$ first migrates to Cp ring from W atom to generate a 16e intermediate **Int1-1**, followed by oxidative addition of H_2 to afford an 18e intermediate **Int2-1**, then one hydride is bonded to the methylene carbon atom to generate an intermediate **Int3-1**, and finally the $SiMe_3$ returns to the metal from Cp ring to give the product **P**. In Path II, H_2 is coordinated to the metal with the Cp ring slipping from η^5 to η^3 coordination, giving a non-classic H_2 complex **Int1-2**, then conversion of the non-classic H_2 complex to a classic one **Int2-2** is followed, and the product **P** is produced by transferring one hydride to the methylene carbon atom from the metal center. Path III is just a σ-bond metathesis process.

3.1. Theoretical investigation on Path I

The potential energy profile for reaction of **R** with H_2 is shown in Fig. 1a. The geometrical structures involved in Path I, together with structural parameters are illustrated in Fig. 1b. For the first step (**R** to **Int1-1**), reactant **R** undergoes silicon group migration from metal center to the carbon atom of a Cp ring via a transition state **TS1-1** to afford an intermediate **Int1-1**. In **R**, the three-membered W–Si–C ring is theoretically confirmed lying in the symmetric plane of the two Cp rings. The bond angles of Si–W–C, W–Si–C and Si–C–W are calculated to be 43.3°, 60.9°, 75.8°, and the bond distances of W–Si, Si–C and W–C are 2.58, 1.83, 2.33 Å. Obviously, ring strain is involved in the three-membered W–Si–C ring. In **TS1-1**, W–Si bond distance is 2.76 Å, indicating Si atom is being away from the metal center. Si–C2 bond distance is 2.12 Å, while in **R** it is 3.32 Å, indicating Si atom is approaching C2 atom. The W–Si–C ring no longer lies in the symmetric plane of the two Cp rings, and the Si atom approaches the C2 atom of Cp ring. Meanwhile, C2 atom shows a tendency of changing hybridization from sp^2 to sp^3, which leads to C2 atom deviating from the Cp plane. Results of calculations show that the C3–C4–C5–C2 dihedral angle is about 172.7°, and the H atom attached on C2 atom is correspondingly out of the Cp plane. The C3–C4–C5–H1 dihedral angle is calculated to be about 150.7°. W–C1 bond distance (2.24 Å) is smaller than that in **R**, implying the bond is enhanced in **TS1-1**. The release of ring strain involved in the W–Si–C1 ring is responsible for the shorter bond length. In **Int1-1**, coordination of one Cp to W has transformed from η^5 to η^4 mode. The bond distances of

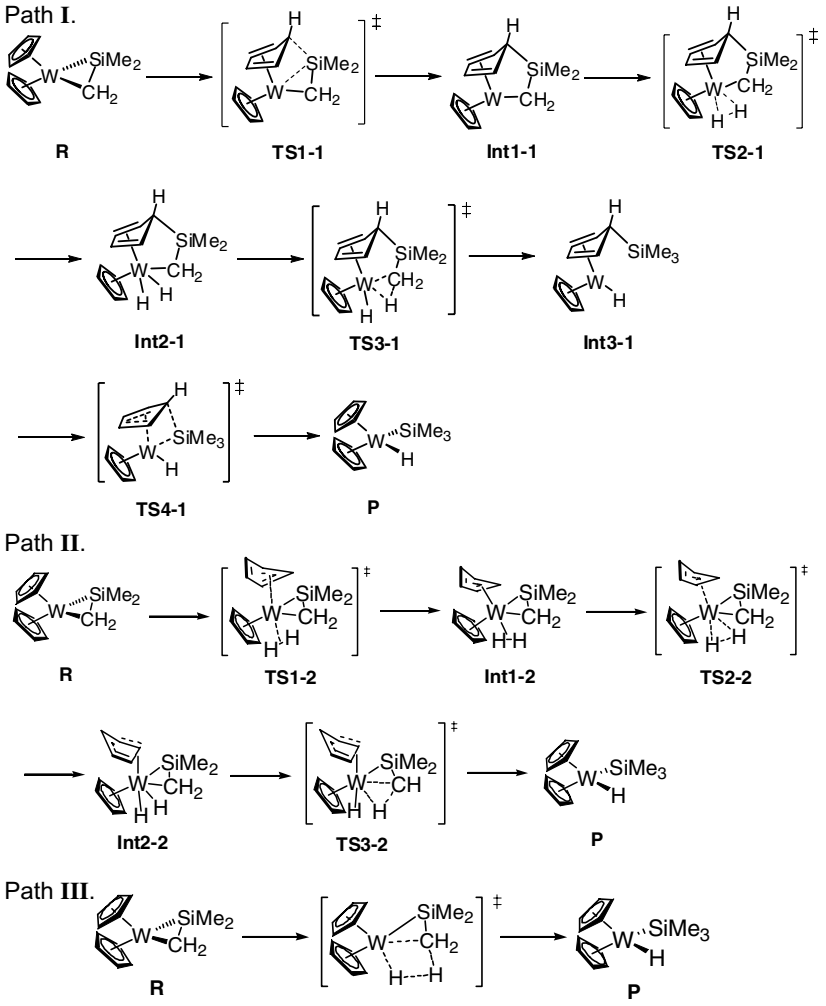

Scheme 1.

W–C3, W–C4, W–C5, W–C6 are almost the same (2.27, 2.20, 2.20, 2.29 Å), while the W–C2 bond is much longer (2.65 Å). The Si–C2 bond is formed (1.92 Å), and the hybridization of C2 changes from sp^2 to sp^3. Obviously, C2 atom coordinates no longer to the metal center but binds to the Si atom, and W–Si bond is cleaved. Further release of ring strain of W–Si–C1 compared with that in **TS1-1** strengthens the W–C1 bond to a larger extent (2.19 Å). The reaction activation energy for this step is calculated to be 17.8 kcal/mol. The calculated energy difference for the step is 12.9 kcal/mol, indicating this step is unfavored thermodynamically. Two major aspects affect the energy difference magnitude. One is the release of ring strain, which is in favor of this step thermodynamically. Another is the transformation of coordination configuration from an 18e species (**R**) to a 16e one (**Int1-1**), which is not favorable for the step. Clearly, the change from 18e to 16e configuration is responsible for the relatively instability of **Int1-1**.

The second step (**Int1-1** to **Int2-1**) is coordination of dihydrogen to W to give a classic tungsten hydride (**Int2-1**). In **TS2-1**, dihydrogen is approaching to W. Calculated W–H2, W–H3 bond distances are 2.48, 2.76 Å, respectively. H2–H3 bond distance is 0.75 Å, longer a little than that calculated for free dihydrogen (0.74 Å). In **Int2-1**, the H2–H3 bond is broken with the bond distance to be 1.78 Å. Both W–H2 and W–H3 bond distances are calculated to be 1.70 Å, respectively, confirming two classic W–H bonds have been formed. Activation energy for this step is calculated to be 4.5 kcal/mol. The calculated energy difference is −19.8 kcal/mol, indicating this step is much favorable thermodynamically. Transformation of 16e to 18e configuration and formation of strong W–H bonds are responsible for the favored thermodynamics.

The third step (**Int2-1** to **Int3-1**) is migration of hydrogen from metal center to methylene carbon atom. In **TS3-1**, W–H3 bond (1.72 Å) is longer, and C1–H3 bond distance (1.52 Å) is shorter than that in **Int2-1**, indicating H3 atom is leaving W for C1 atom. W–C1 (2.44 Å) is longer than that in **Int2-1** (2.30 Å), implying the bond is being broken. Activation energy for the step is calculated to be 14.3 kcal/mol. With bond cleavage of W–C1 and W–H3 and formation of C1–H3 in **Int3-1**, a new methyl group containing C1 atom is formed. **Int3-1** is a coordina-

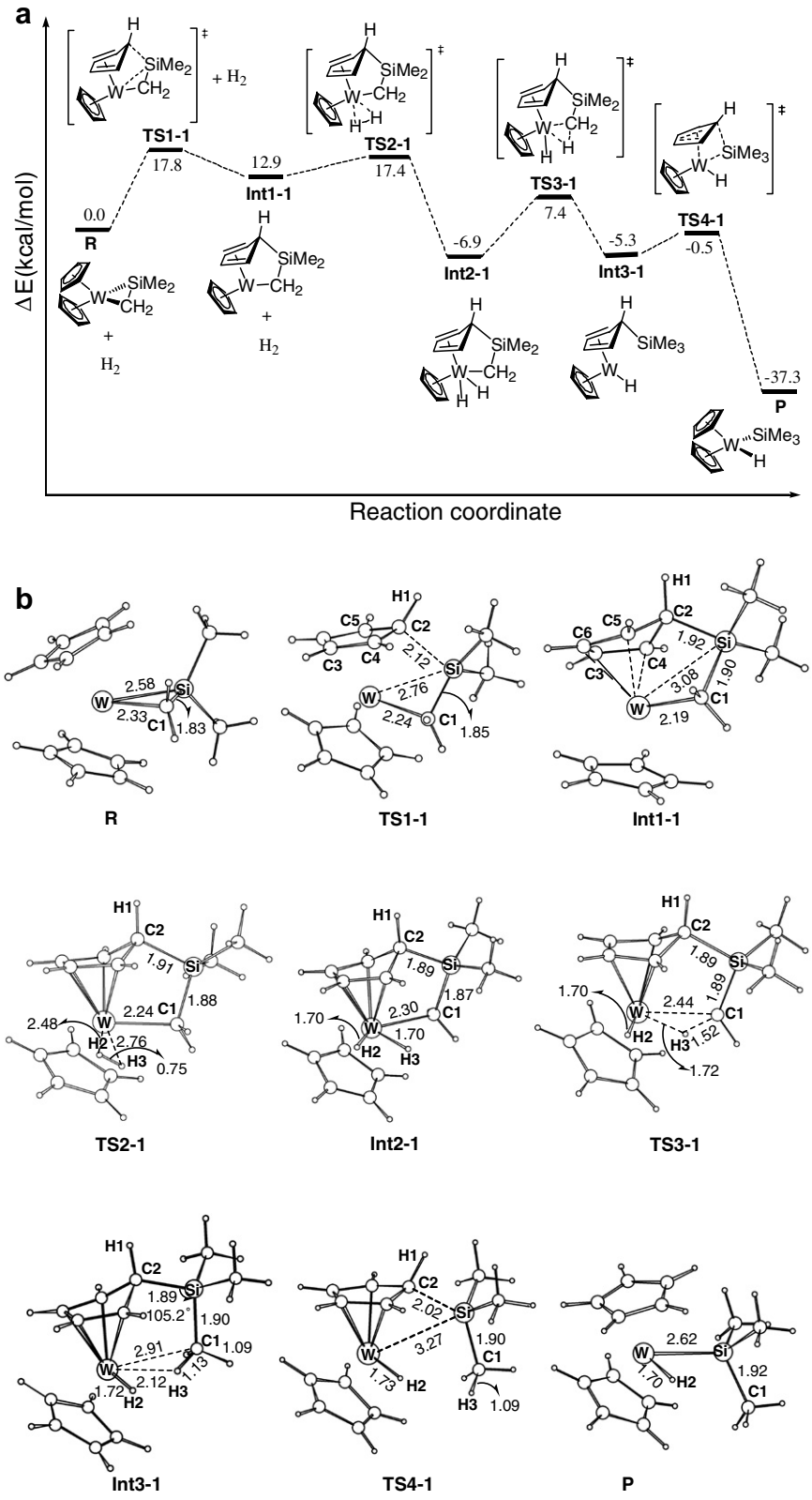

Fig. 1. (a) Potential energy profile of the first possible pathway for reaction of **R** with H_2. The energies are given in kcal/mol. (b) B3LYP optimized structures of the species involved in Path I with selected structural parameters. The bond lengths are given in Å.

tion-unsaturated 16e species. Carefully examining its geometrical structure, we find the C1–H3···W agostic interaction is involved. Several aspects are presented in evidence. (i) In terms of steric hindrance, it seems better for the methyl ($C1H_3$) being away from metal center. However, it is found that calculated W–H3 distance is only 2.12 Å,

implying H3 atom is much close to metal center. (ii) Calculated C1–H3 bond length is 1.13 Å, while the other C1–H bond lengths are 1.09 Å. That means the C1–H3 σ-bond is weakened and the other two keep unchangeable. (iii) C2–Si–C1 bond angle is calculated to be 105.2° while the other two C–Si–C1 bond angles are about 109.5°. The smaller C2–Si–C1 bond angle also supports the occurrence of agostic interaction between metal center and C1–H3 bond. (iv) Energy difference for the step is calculated to be only 1.6 kcal/mol. **Int2-1**(18e) is more stable a little than **Int3-1** (16e). Certainly, stability of the 16e **Int3-1** is enhanced with the occurring agostic interaction. (v) **R** is an 18e species and **Int3-1** is a 16e species. Generally, 18e species are more stable than 16e species. However, **Int3-1** is even more stable than **R**. Two factors are given to explain the phenomenon. One is the ring strain involved in **R** which weakens its stability. The other is the agostic interaction mentioned above which enhances the stability of **Int3-1**. On the basis of the evidence present above, we confirmed the involvement of agostic interaction between W and C1–H3.

The last step (**Int3-1** to **P**) is the silicon group going back to metal center from C2 via **TS4-1**. The Si–C2 bond distance (2.02 Å) in **TS4-1** is longer than that (1.89 Å) in **Int3-1**, indicating Si atom is leaving C2 atom. The W–Si bond distance (3.27 Å) in **TS4-1** is shorter than that (3.61 Å) in **Int3-1**, indicating Si is approaching to the metal center. The W–H3 distance becomes much longer (3.45 Å) than that (2.12 Å) in **Int3-1**, and the C1–H3 bond resumes its normal length (1.09 Å) from 1.13 Å, indicating the agostic interaction mentioned above is no longer existent. The activation energy for this step is calculated to be only 4.8 kcal/mol, implying this kind of migration is relatively labile. In the product **P**, the silicon group moves to metal center from C2 atom. The calculated W–Si length is 2.62 Å. The calculated energy difference for the step is −32.0 kcal/mol, indicating this step is much favorable thermodynamically. Transformation from 16e to 18e configuration is mainly responsible for favored thermodynamics.

For the whole Path I, it can be predicted from Fig. 1a that both the migration of the silicon group from metal center to C2 (step 1) and the coordination of dihydrogen to metal center are theoretically predicted to be the rate-determining steps. The reaction studied here is significantly thermodynamic favorable confirmed by the calculated reaction energy difference (−37.3 kcal/mol). Relief of ring strain, formation of new C1–H3 and W–H2 bonds contribute to the stability of **P**.

3.2. Theoretical investigation on Path II

The potential energy profile for reaction of **R** with H_2 is shown in Fig. 2a. The geometrical structures involved in Path II, together with structural parameters are illustrated in Fig. 2b. Step 1 (**R** to **Int1-2**) in Fig. 2a is a process of the Cp ring slippage. One of the Cp rings moves from an η^5 to an η^3 coordination. As shown by the geometrical structure of **Int1-2**(Fig. 2 (b)), a molecular dihydrogen complex is afforded with a Cp ligand coordinated to W in a trihapto form. The W–H1 and W–H2 bond distance are calculated to be 1.83 Å and 1.90 Å, respectively, and the H1–H2 bond length (0.86 Å) becomes longer than the free H–H (0.74 Å) bond length, indicating H_2 bonded to the metal in a non-classic η^2 form. For avoiding appearance of 20e species, one Cp ring undergoes ring slip from η^5 to η^3 to follow 18e rule. As shown in **Int1-2**, C5, C6 are far away from metal while C2, C3 and C4 stay close to the metal. C2–C3 and C3–C4 keep their bond lengths (1.43 Å) almost unchanged, while C5–C6 returns to a nearly normal C=C double bond (1.36 Å), suggesting coordination of the Cp ring changing from η^5 to η^3. The energy difference for this step is calculated to be 32.3 kcal/mol, indicating much unfavorable thermodynamically. The reason for instability of the intermediate is that the H_2 binding to the metal is quite weak and the coordination of Cp is much stronger in an η^5 form than in an η^3 form. In **TS1-2**, the W–C5 and W–C6 bonds are longer than those in **R** and shorter than those in **Int1-2**. W–H1 and W–H2 are longer than those in **Int1-2** and the H1–H2 bond distance (0.76 Å) is in between **Int1-2**(0.86 Å) and its free form (0.74 Å), suggesting H_2 is coordinating to the metal center. The activation energy for H_2 coordination in an η^2 form is calculated to be 36.5 kcal/mol, indicating much unfavorable kinetically.

The second step (**Int1-2** to **Int2-2**) is transformation of a non-classic complex to a classic one. Compared with the non-classic H_2 complex **Int1-2**, the H1–H2 bond is broken, supported by the calculated structural data (Fig. 2b). The H1–H2 distance in **Int2-2** changes to 1.92 Å from 0.86 Å in **Int1-2** and the W–H1 and W–H2 bonds become much shorter (1.69 Å, 1.69 Å) compared to those in **Int1-2**(1.83 Å, 1.90 Å). That means two metal-hydride bonds are formed. The energy difference for this step is calculated to be −9.4 kcal/mol. Obviously, the binding of the metal with the two hydrogen atoms in **Int2-2** is stronger than in **Int1-2**. The higher stability of **Int2-2** compared with **Int1-2** is due to formation of the two strong W–H bonds. In the transition state **TS2-2** connecting both the intermediates, the W–H1, W–H2 and H1–H2 bond distances are calculated to be reasonably in between **Int1-2** and **Int2-2**, which indicates the H1–H2 bond is being broken to afford the metal hydride complex. The barrier for this step is calculated to be only 0.3 kcal/mol, implying this step is very much favored kinetically.

Step 3 is the hydrogen migration from the metal to the methylene C atom. In **TS3-2**, the W–H2 and W–C1 are elongated and the H2 becomes closer to C1 compared with those in **Int2-2**. In the product **P**, H2 forms a σ-bond with C1 and the W–C1 bond is cleaved. The calculated barrier for the step is 13.9 kcal/mol. The energy difference is calculated for this step to be −60.2 kcal/mol, indicating this step is much favorable thermodynamically. The reason for the higher stability of **P** compared with the intermediate **Int2-2** is that (i) the η^5 coordination of Cp ring in **P** is much stronger than the η^3 coordination of that in **Int2-2**, and

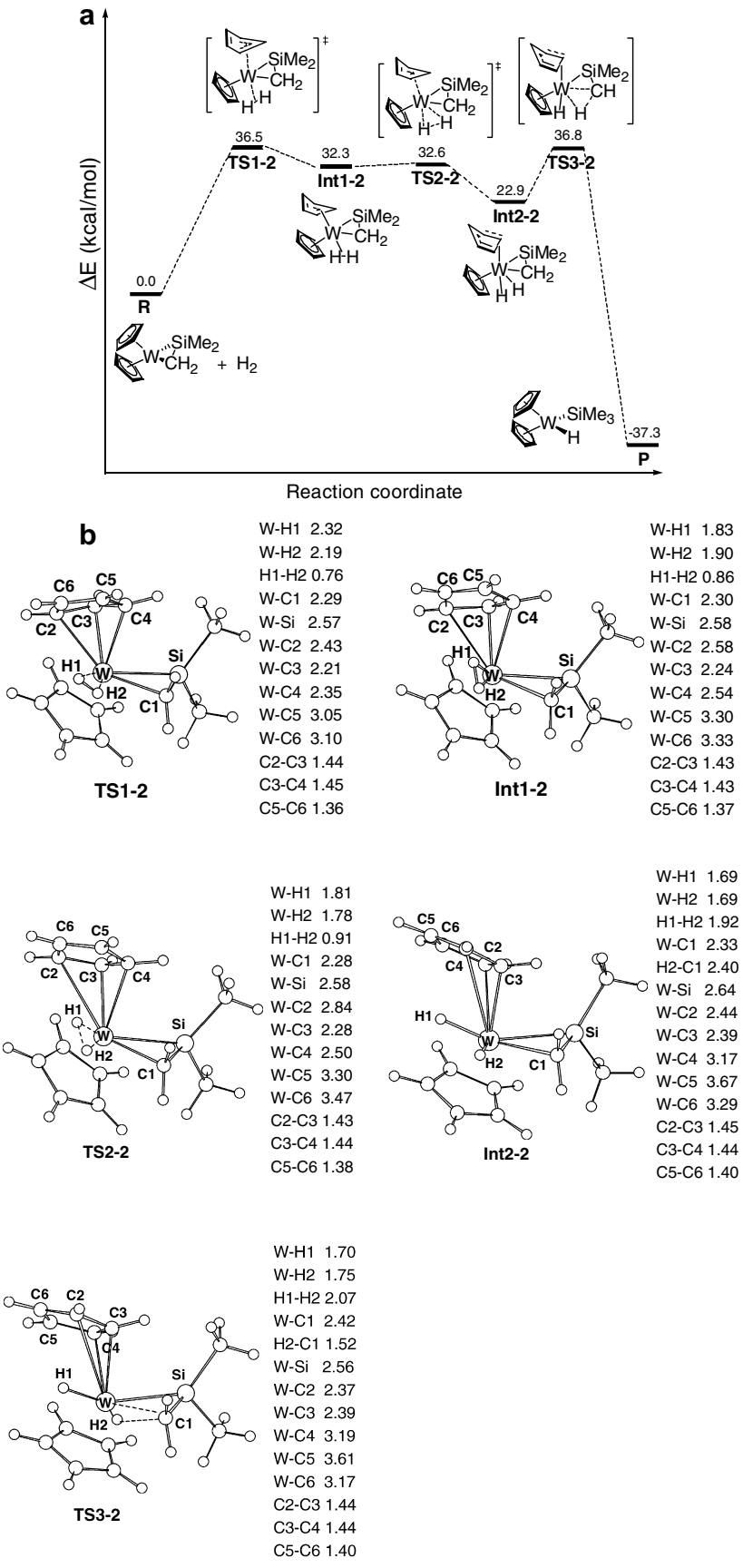

Fig. 2. (a) Potential energy profile of Path II for reaction of **R** with H_2. The energies are given in kcal/mol. (b) B3LYP optimized structures of the species involved in Path II with selected structural parameters. The bond lengths are given in Å.

(ii) the W–Si–C1 ring strain is released from **Int2-2** to **P** due to the W–C1 bond cleavage. The high activation energy for Path II implies the pathway undergoing Cp ring slippage is much disfavored kinetically.

Path III is proposed on the basis of the fact that the two Cp rings and the CH_2=$SiMe_2$ unit are bonded to the metal center strongly, which means it is difficult to lose a ligand to generate a 16e intermediate for the purpose of coordination of H_2. Obviously, H_2 cannot directly coordinate to the metal to lead to a 20e species. Therefore, one alternative possible pathway to obtain the product is by σ-bond metathesis between W–C and H–H. However, we spent much time to locate the transition state associated with the σ-bond metathesis, but we failed. We predict that Path III may not exist.

It can be seen clearly from Fig. 1a and Fig. 2a that Path I is much more favorable kinetically than Path II, which is in agreement with the experimental proposal. The maximal activation energy for Path I is calculated to be just over 17 kcal/mol, while that for Path II is over 36 kcal/mol. In summary, in this reaction, migration of silicon group is kinetically favorable, while the pathways involving Cp slippage and σ-bond metathesis are not, respectively. The relatively low reaction activation energy in Path I is caused mainly by relief of ring strain in generating the intermediate **Int1-1**. The much higher reaction activation energy in Path II is due to the instability of η^3-coordinated complexes.

4. Conclusions

Experiments confirmed that $Cp_2W(\eta^2\text{-}Me_2Si{=}CH_2)$ (**R**) could react with H–X (X=H, $SiMe_3$) to afford the products $Cp_2WX(SiMe_3)$. In this paper, we adopt the reaction of **R** with H_2 as a model to theoretically explore the mechanisms of such reactions by using density functional theory (DFT). As a result of the fact that **R** is an 18e species and difficult to lose a ligand to create a vacant site for coordination of the substrates like H_2 and $HSiMe_3$, three possible pathways are proposed based on the features of the model reaction and the experimental proposal. The first two paths are based on the idea of first creating a vacant site and then followed by coordination of H_2. One way is to create a vacant site by migration of silicon group from metal to Cp ring. The second way to generate a vacant site is by Cp ring slippage from η^5 to η^3-coordination. The third path is based on σ-bond metathesis. Our results of calculations indicate that Path I is the most favored, which is in agreement with the experimental proposal. That is, migration of silicon group from W to Cp ring is involved in the reaction. Relief of ring strain in affording the 16e **Int1-1** is mainly responsible for the kinetically favored pathway.

Acknowledgement

This work was supported by the National Natural Science Foundation of China (No.: 20473047).

References

[1] B.K. Campion, R. Heyn, T.D. Tilley, J. Am. Chem. Soc. 110 (1988) 7558.
[2] B.K. Campion, R. Heyn, T.D. Tilley, J. Am. Chem. Soc. 112 (1990) 4079.
[3] T.S. Koloski, P.J. Carroll, D.H. Berry, J. Am. Chem. Soc. 112 (1990) 6405.
[4] E.K. Pham, R.J. West, J. Am. Chem. Soc. 111 (1989) 7667.
[5] E.K. Pham, R. West, Organometallics 9 (1990) 1517.
[6] D.H. Berry, J.H. Chey, H.S. Zipin, P.J. Carroll, J. Am. Chem. Soc. 112 (1990) 452.
[7] S.R. Klei, T.D. Tilley, R.G. Bergman, Organometallics 20 (2001) 3220.
[8] S. Kuroda, F. Dekura, Y. Sato, M. Mori, J. Am. Chem. Soc. 123 (2001) 4139.
[9] Michael Bendikov, Sabine Ruth Quadt, Oded Rabin, Yitzhak Apeloig, Organometallics 21 (2002) 3930.
[10] M.S. Eisen, in: Z. Rappoport, Y. Apeloig (Eds.), The Chemistry of Organic Silicon Compounds, vol. 2, Wiley, New York, 1998, p. 2037 (Chapter 35).
[11] T.D. Tilley, in: S. Patai, Z. Rappoport (Eds.), The Silicon–Heteroatom Bond, Wiley, New York, 1991, pp. 245–309 (Chapters 9 and 10).
[12] T.S. Koloski, D.C. Pestana, P.J. Carroll, D.H. Berry, Organometallics 13 (1994) 489.
[13] S.R. Berryhill, G.L. Clevenger, F.Y. Burdurlu, Organometallics 4 (1985) 1509.
[14] G.L. Crocco, C.S. Young, K.E. Lee, J.A. Gladysz, Organometallics 7 (1988) 2158.
[15] U. Schubert, A. Schenkel, Chem. Ber. 121 (1988) 939.
[16] J.M. O'connor, C.P. Casey, Chem. Rev. 87 (1987) 307.
[17] C.P. Casey, J.M. O'Connor, W.D. Jones, K.J. Haller, Organometallics 2 (1983) 535.
[18] T.R. Cundari, J. Am. Chem. Soc. 114 (1992) 10557.
[19] A. Milet, A. Dedieu, G. Kapteijn, G. Koten, Inorg Chem. 36 (1997) 3223.
[20] C. Lee, W. Yang, G. Parr, Phys. Rev. B 37 (1988) 785.
[21] B. Miehlich, A. Savin, H. Stoll, H. Preuss, Chem. Phys. Lett. 157 (1989) 200.
[22] A.D. Becke, J. Phys. Chem. 98 (1993) 5648.
[23] K. Fukui, J. Phys. Chem. 74 (1970) 4161.
[24] K. Fukui, Acc. Chem. Res. 14 (1981) 363.
[25] P.J. Hay, W.R. Wadt, J. Chem. Phys. 82 (1985) 299.
[26] (a) S. Bi, Z. Lin, R.F. Jordan, Organometallics 23 (2004) 4882;
(b) S. Bi, A. Ariafard, G. Jia, Z. Lin, Organometallics 24 (2005) 680;
(c) A. Ariafard, S. Bi, Z. Lin, Organometallics 24 (2005) 2241;
(d) A. Ariafard, Z. Lin, Organometallics 24 (2005) 3800;
(e) J. Zhu, G. Jia, Z. Lin, Organometallics 25 (2006) 1812;
(f) A. Ariafard, Z. Lin, Organometallics 25 (2006) 4030;
(g) A. Ariafard, Z. Lin, J. Am. Chem. Soc. 128 (2006) 13010;
(h) A. Ariafard, Z. Lin, J.S. Fairlamb, Organometallics 25 (2006) 5788;
(i) H. Zhao, Z. Lin, T.B. Marder, J. Am. Chem. Soc. 128 (2006) 15637.